J Solid State Electrochem (2007) 11:1643–1653
DOI 10.1007/s10008-007-0324-2

ORIGINAL PAPER

An electrochemical investigation on the reduction path of the arene complexes $[CpM(arene)]^{2+}$ and $[(\eta\text{-}9\text{-}SMe_2\text{-}7,8\text{-}C_2B_9H_{10})M(arene)]^{2+}$ (M=Rh, Ir)

Maddalena Corsini · Serena Losi · Emanuela Grigiotti · Fulvio Rossi · Piero Zanello · Alexander R. Kudinov · Dmitry A. Loginov · Mikhail M. Vinogradov · Zoya A. Starikova

Received: 22 September 2006 / Revised: 22 November 2006 / Accepted: 28 November 2006 / Published online: 28 April 2007

Abstract The reduction behavior of the isoelectronic complexes $[CpM^{III}(\eta^6\text{-}C_6R_6)]^{2+}$ (M=Rh, Ir; R=H, Me) and $[(\eta\text{-}9\text{-}SMe_2\text{-}7,8\text{-}C_2B_9H_{10})M^{III}(\eta^6\text{-}C_6R_6)]^{2+}$ (M=Rh, Ir; C_6R_6=C_6H_6, C_6H_5OMe, $C_6H_3Me_3$) has been studied by cyclic voltammetry and controlled potential coulometry in acetonitrile and propylene carbonate at 253 and 298 K, respectively. The extent of chemical reversibility of the pertinent sequences Rh(III)/Rh(II)/Rh(I) and Ir(III)/Ir(I) is highly dependent on both the nature of the solvent and the intrinsic electronic properties of the arene substituents. The arene η^6 coordination makes the derivatives in their lower oxidation states notably short lived, even if, in some cases, the use of propylene carbonate improves their stability or causes the increase in their lifetimes before changing the arene coordination from η^6 to η^4. Cations $[(\eta\text{-}9\text{-}SMe_2\text{-}7,8\text{-}C_2B_9H_{10})M(\eta^6\text{-}C_6R_6)]^{2+}$ were obtained by the bromide abstraction from $[(\eta\text{-}9\text{-}SMe_2\text{-}7,8\text{-}C_2B_9H_{10})MBr_2]_2$ with Ag^+ in the presence of benzene and its derivatives. The structure of $[(\eta\text{-}9\text{-}SMe_2\text{-}7,8\text{-}C_2B_9H_{10})Ir(\eta^6\text{-}C_6H_5OMe)](BF_4)_2$ was determined by X-ray diffraction.

M. Corsini · S. Losi · E. Grigiotti · F. Rossi · P. Zanello (✉)
Dipartimento di Chimica, Università di Siena,
Via Aldo Moro,
53100 Siena, Italy
e-mail: zanello@unisi.it

A. R. Kudinov · D. A. Loginov · M. M. Vinogradov · Z. A. Starikova
A. N. Nesmeyanov Institute of Organoelement Compounds,
Russian Academy of Sciences, GSP-1, Russian Federation,
28 ul. Vavilova,
119991 Moscow, Russia

A. R. Kudinov
e-mail: arkudinov@ineos.ac.ru

Keywords Rh(III) and Ir(III) complexes · Cyclopentadienyl/arene sandwich ligands · Cyclopentadienyl/carborane sandwich ligands · X-ray crystal structure · Electrochemistry

Introduction

The electrochemical behavior of a few members of the series $[(\eta^5\text{-}C_5R_5)M^{III}(\eta^6\text{-}C_6R_6)]^{2+}$ (M=Rh, Ir) is long known [1, 2]. The η^6-coordinated arene Rh(III) dications [3] undergo the stepwise sequence Rh(III)/Rh(II)/Rh(I) [1, 2], which ultimately convert them to the η^4-coordinated arene Rh(I) species $[(\eta^5\text{-}C_5R_5)M(\eta^4\text{-}C_6R_6)]^0$ [2] through the generally short-lived Rh(II) intermediates $[(\eta^5\text{-}C_5R_5)M(\eta^6\text{-}C_6R_6)]^+$. In contrast, the Ir(III) derivatives undergo the single-step process Ir(III)/Ir(I) [1].

As in both cases the reduction processes display different extents of chemical reversibility depending upon the nature of the solvent (acetonitrile vs acetone) [1, 2], and in view of the stability of the Co(III)/Co(II)/Co(I) sequence for the $[(\eta^5\text{-}C_5R_5)Co^{III}(\eta^6\text{-}C_6R_6)]^{2+}$ analogues in propylene carbonate (PC) solution [4], we have compared the redox activity of the isoelectronic complexes $[CpM(\eta^6\text{-}C_6R_6)]^{2+}$ (R=H, Me) and $[(\eta\text{-}9\text{-}SMe_2\text{-}7,8\text{-}C_2B_9H_{10})M(\eta^6\text{-}C_6R_6)]^{2+}$ (C_6R_6=C_6H_6, C_6H_5OMe, $C_6H_3Me_3$), Scheme 1, in acetonitrile solution, in which their redox intermediates are typically unstable, with respect to that in propylene carbonate solution.

Materials and methods

The synthesis of the complexes was carried out under an inert atmosphere in dry solvents. The isolation of products

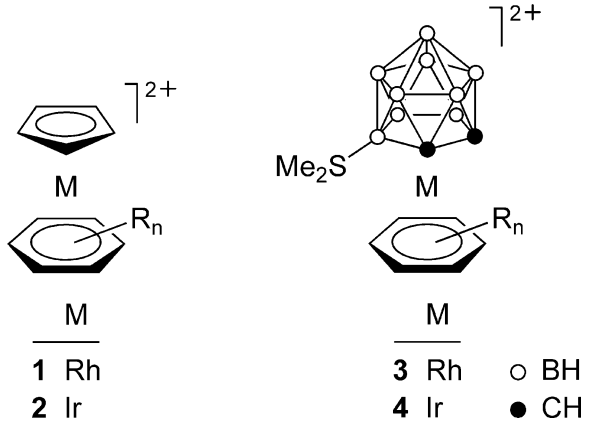

Scheme 1 Arene complexes studied in the present work

was conducted in air. Complexes **1a**,**e** and **2a**,**e** [3] and starting materials $[(\eta\text{-}9\text{-}SMe_2\text{-}7,8\text{-}C_2B_9H_{10})RhBr_2]_2$ [5], $[(\eta\text{-}9\text{-}SMe_2\text{-}7,8\text{-}C_2B_9H_{10})IrBr_2]_2$ [6], and $AgBF_4{\cdot}3$dioxane [7] were prepared as described in the literature. ^1H and $^{11}B\{^1H\}$ nuclear magnetic resonance (NMR) spectra (δ in ppm) were recorded on a Bruker AMX-400 spectrometer (^1H 400.13; ^{11}B 128.38 MHz) relative to residual protons of the solvents (^1H) or $BF_3{\cdot}Et_2O$ (^{11}B, external standard).

Materials and apparatus for electrochemistry have been described elsewhere [8]. Potential values are referred to the saturated calomel electrode.

The analysis of the cyclic voltammetric responses was carried out in a non-isothermic cell in the scan rate range from 0.02 to 50 V s^{-1} at the temperatures of 298 and 253 K, respectively.

Under the present experimental conditions, the one-electron oxidation of ferrocene at 298 K occurs at $E^{\circ\prime}$= +0.38 V (ΔE_p=64 mV at 0.2 V s^{-1}) in MeCN and at $E^{\circ\prime}$= +0.37 V (ΔE_p=67 mV at 0.2 V s^{-1}) in PC.

Synthesis of complexes $[(\eta\text{-}9\text{-}SMe_2\text{-}7,8\text{-}C_2B_9H_{10})M(arene)](BF_4)_2$ (**3**$(BF_4)_2$ and **4**$(BF_4)_2$)

$MeNO_2$ (2 ml) was added to a mixture of $[(\eta\text{-}9\text{-}SMe_2\text{-}7,8\text{-}C_2B_9H_{10})MBr_2]_2$ (M=Rh, Ir; 0.064 mmol), $AgBF_4{\cdot}3$dioxane (0.259 mmol), and arene (0.7 ml of benzene, *m*-xylene, mesitylene, or anisole; 120 mg durene or hexamethylbenzene). The reaction mixture was stirred for about 24 h, and the precipitate of AgBr was centrifuged off. The solvent was removed in vacuo. The residue was re-precipitated from nitromethane by CH_2Cl_2 to give white solids.

3a $(BF_4)_2$ M=Rh, arene=C_6H_6. The precipitate obtained was thoroughly washed with ether to remove admixture of $MeNO_2$. Yield 56%. Anal. Calc. for $C_{10}H_{22}B_{11}F_8RhS$: C, 21.91; H, 4.05; B, 21.69%. Found: C, 21.07; H, 3.89; B, 21.14%. $^{11}B\{^1H\}$ NMR (nitromethane-d_3): δ=16.5 (1B), 13.7 (1B), 7.9 (1B), 4.4 (1B), 0.2 (1B), −1.5 (2B, BF_4^-), −3.7 (1B), −9.9 (1B), −11.9 (1B), −18.1 (1B).

3b $(BF_4)_2$M=Rh, arene=1,3-$C_6H_4Me_2$. Yield 37%. Anal. Calc. for $C_{12}H_{26}B_{11}F_8RhS$: C, 25.01; H, 4.55; B, 20.64%. Found: C, 24.83; H, 4.41; B, 20.64%. $^{11}B\{^1H\}$ NMR (nitromethane-d_3): δ=14.9 (2B), 6.7 (1B), 5.5 (1B), −0.5 (1B), −1.4 (2B, BF_4^-), −3.9 (1B), −10.3 (1B), −12.1 (1B), −18.6 (1B).

3c $(BF_4)_2$M=Rh, arene=1,3,5-$C_6H_3Me_3$. Yield 53%. Anal. Calc. for $C_{13}H_{28}B_{11}F_8RhS$: C, 26.45; H, 4.78; B, 20.15%. Found: C, 26.37; H, 4.68; B, 20.15%. $^{11}B\{^1H\}$ NMR (nitromethane-d_3): δ=16.2 (1B), 14.1 (1B), 5.9 (1B), 4.3 (1B), −0.9 (1B), −1.4 (2B, BF_4^-), −4.1 (1B), −10.4 (1B), −12.0 (1B), −18.7 (1B).

3d $(BF_4)_2$M=Rh, arene=1,3,4,5-$C_6H_2Me_4$. The oily product cannot be obtained in analytically pure form. $^{11}B\{^1H\}$ NMR (nitromethane-d_3): δ=15.8 (1B), 13.0 (1B), 6.6 (1B), 5.8 (1B), −1.5 (2B, BF_4^-), −2.0 (1B), −4.3 (1B), −10.7 (1B), −12.2 (1B), −18.7 (1B).

3e $(BF_4)_2$M=Rh, arene=C_6Me_6. The oily product cannot be obtained in analytically pure form. $^{11}B\{^1H\}$ NMR (nitromethane-d_3): δ=15.5 (1B), 11.5 (1B), 7.5 (1B), 3.7 (1B), −1.5 (2B, BF_4^-), −3.0 (1B), −4.5 (1B), −10.6 (1B), −12.1 (1B), −20.0 (1B).

3f $(BF_4)_2$M=Rh, arene=C_6H_5OMe. Yield 72%. Anal. Calc. for $C_{11}H_{24}B_{11}F_8ORhS$: C, 22.85; H, 4.18; B, 20.57%. Found: C, 22.03; H, 4.08; B, 20.35%. $^{11}B\{^1H\}$ NMR (nitromethane-d_3): δ=14.5 (1B), 13.0 (1B), 6.4 (1B), 4.3 (1B), −0.7 (1B), −1.5 (2B, BF_4^-), −4.4 (1B), −10.7 (1B), −12.7 (1B), −18.8 (1B).

4a $(BF_4)_2$M=Ir, arene=C_6H_6. Yield 78%. Anal. Calc. for $C_{10}H_{22}B_{11}F_8IrS$: C, 18.84; H, 3.48; B, 18.66%. Found: C, 18.98; H, 3.49; B, 18.48%. $^{11}B\{^1H\}$ NMR (nitromethane-d_3): δ=11.7 (1B), 1.6 (1B), 0.1 (1B), −1.5 (2B, BF_4^-), −4.6 (2B), −8.3 (1B), −15.2 (1B), −16.7 (1B), −21.6 (1B).

4b $(BF_4)_2$M=Ir, arene=1,3-$C_6H_4Me_2$. Yield 41%. Anal. Calc. for $C_{12}H_{26}B_{11}F_8IrS$: C, 21.66; H, 3.94; B, 17.87%. Found: C, 21.44; H, 3.91; B, 17.69%. $^{11}B\{^1H\}$ NMR (nitromethane-d_3): δ=10.5 (1B), 3.1 (1B), −0.6 (1B), −1.5 (2B, BF_4^-), −3.7 (1B), −5.0 (1B), −8.4 (1B), −15.4 (1B), −16.7 (1B), −21.5 (1B).

4c $(BF_4)_2$M=Ir, arene=1,3,5-$C_6H_3Me_3$. Yield 71%. Anal. Calc. for $C_{13}H_{28}B_{11}F_8IrS$: C, 22.98; H, 4.15; B, 17.50%. Found: C, 22.79; H, 4.28; B, 16.45%. $^{11}B\{^1H\}$ NMR (nitromethane-d_3): δ=10.0 (1B), 4.4 (1B), −1.0 (1B), −1.5 (2B, BF_4^-), −5.3 (2B), −8.5 (1B), −15.5 (1B), −16.5 (1B), −21.6 (1B).

4d $(BF_4)_2$M=Ir, arene=1,3,4,5-$C_6H_2Me_4$. Yield 55%. Anal. Calc. for $C_{14}H_{30}B_{11}F_8IrS$: C, 24.24; H, 4.36; B, 17.15%. Found: C, 24.04; H, 4.27; B, 16.74%. $^{11}B\{^1H\}$ NMR (nitromethane-d_3): δ=9.3 (1B), 4.0 (1B), −0.9 (1B), −1.5

(2B, BF_4^-), −2.2 (1B), −5.2 (1B), −8.4 (1B), −15.5 (1B), −16.9 (1B), −21.6 (1B).

4e$(BF_4)_2$M=Ir, arene=C_6Me_6. The oily product cannot be obtained in analytically pure form. $^{11}B\{^1H\}$ NMR (nitromethane-d_3): δ=8.1 (1B), 3.8 (1B), −1.5 (2B, BF_4^-), −2.5 (1B), −5.8 (1B), −7.1 (1B), −8.6 (1B), −15.7 (1B), −17.0 (1B), −21.1 (1B).

4f$(BF_4)_2$ M=Ir, arene=C_6H_5OMe. Yield 80%. Anal. Calc. for $C_{11}H_{24}B_{11}F_8OIrS$: C, 19.79; H, 3.62; B, 17.82%. Found: C, 19.78; H, 3.61; B, 17.75%. $^{11}B\{^1H\}$ NMR (nitromethane-d_3): δ=10.4 (1B), 1.2 (1B), −0.9 (1B), −1.5 (2B, BF_4^-), −5.2 (2B), −8.8 (1B), −15.7 (1B), −17.0 (1B), −21.8 (1B).

Arene exchange in [(η-9-SMe_2-7,8-$C_2B_9H_{10}$)Rh(η-C_6H_6)]$(BF_4)_2$ (**3a**$(BF_4)_2$)

Anisole (0.1 ml, 0.923 mmol) was added to solution of **3a**$(BF_4)_2$ (37 mg, 0.041 mmol) in nitromethane (2 ml). The reaction mixture was refluxed for 2 h. Ether (about 8 ml) was added to precipitate white complex **3f**$(BF_4)_2$ identified by ^1H NMR spectrum. Yield 26 mg (66%).

X-ray crystallography of [(η-9-SMe_2-7,8-$C_2B_9H_{10}$)Ir(η-C_6H_5OMe)]$(BF_4)_2$ (**4f**$(BF_4)_2$)

Crystals of **4f**$(BF_4)_2$ were grown up by slow diffusion in two-layer system, ether, and a solution of complex in nitromethane and were stored under light petroleum ether. Crystal data: $C_{11.5}H_{25}B_{11}F_8IrOS$ (M=674.48, solvate with 0.083 mol of C_6H_{12}), rhombohedral, space group *R-3*, $a=b$= 15.6195(12), c=48.846(5) Å, γ=120.00°, V=10320.4 (16) Å^3, Z=18, d_{calc}=1.953 g cm^{-3}, μ=5.982 mm^{-1}, F (000)=5,796, yellow plate, crystal size 0.55×0.40× 0.25 mm.

X-ray diffraction experiment was carried out with a Bruker SMART 1000 CCD area detector, using graphite monochromated Mo Kα radiation (λ=0.71073 Å, ω scans with a 0.3° step in ω and 10 s per frame exposure, 3.71<θ< 29.43°) at 120 K. Low temperature of the crystal was maintained with a Cryostream (Oxford Cryosystems) open-flow N_2 gas cryostat. Reflection intensities were integrated using SAINT software, and absorption correction was applied semi-empirically using SADABS program (T_{max}/ T_{min}=0.246/0.090). The structure was solved by direct method and refined by the full-matrix least-squares technique against F^2 in anisotropic approximation for non-hydrogen atoms. The hydrogen H(B) and H(C) positions in the carborane fragment were located from the Fourier synthesis, the positions of H(Me) and H(C_6H_5) atoms were calculated. All hydrogen atoms were refined in the isotropic approximation in riding model with the U_{iso}(H) parameters equal to 1.2U_{eq}(C_i) or 1.5U_{eq}(C_{ii}), where U(C_i) and U(C_{ii}) are, respectively, the equivalent thermal parameters of the methyne and methyl carbon atoms to which the corresponding H atoms are bonded. The refinement converged to wR_2=0.0777 and GOF=1.003 for all independent reflections [R_1=0.0299 was calculated against F for 2,702 observed reflections with $I>2\sigma(I)$], 347 independent parameters. All calculations were performed using the SHELXTL software.

The crystallographic data, atomic coordinates, bond lengths, bond angles, and thermal parameters for **4f**$(BF_4)_2$ have been deposited with the Cambridge Crystallographic Data Center, CCDC-620221. Copies of this information may be obtained free of charge from: The Director, CCDC, 12 Union Road, Cambridge, CB2 1EZ, UK (Fax: +44-1223-336-033; e-mail: deposit@ccdc.cam.ac.uk or http://www.ccdc.cam.ac.uk).

Results and discussion

Synthesis and reactivity

The cyclopentadienyl–arene complexes **1a**,**e** and **2a**,**e** were prepared by reaction of labile nitromethane solvates [CpM$(MeNO_2)_3]^{2+}$ with benzene and hexamethylbenzene, Scheme 2 [3]. The intermediate solvate complexes were obtained by iodide abstraction from $[CpMI_2]_2$.

The monoanionic carborane ligand [9-SMe_2-7,8-$C_2B_9H_{10}]^-$ is analogous to Cp^- in coordinating ability, resulting in similarity of their organometallic derivatives [5, 9–11]. In particular, the reactivity of the halide complexes [(η-9-SMe_2-7,8-$C_2B_9H_{10}$)$MX_2]_2$ (M=Rh, Ir) proved to be

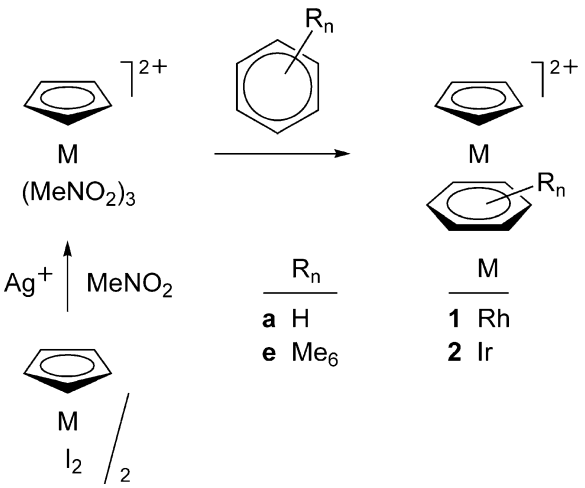

Scheme 2 Synthesis of the cyclopentadienylarene complexes **1a**,**e** and **2a**,**e**

similar to that of $[CpMX_2]_2$ [5, 6, 12, 13]. We found that the bromide abstraction from $[(\eta\text{-}9\text{-}SMe_2\text{-}7,8\text{-}C_2B_9H_{10})MBr_2]_2$ by Ag^+ in the presence of benzene and its derivatives results in dicationic metallacarborane arene complexes **3** and **4**, Scheme 3. The intermediate solvates $[(\eta\text{-}9\text{-}SMe_2\text{-}7,8\text{-}C_2B_9H_{10})M(MeNO_2)_3]^{2+}$ are not stable at room temperature making impossible their preliminary preparation (in contrast to $[CpM(MeNO_2)_3]^{2+}$), explaining inability to obtain analytically pure polymethylated complexes **3d**,**e** and **4e** having low formation rate. The use of other solvents (THF, Me_2CO) instead of nitromethane did not give the target products.

Complexes **3** and **4** are the first examples of dicationic metallacarborane arene complexes. They undergo nucleophilic degradation by coordinating solvents such as Me_2CO and MeCN. The rate of these reactions is considerably higher than in the case of cyclopentadienyl analogues **1** and **2**. For example, according to ^{1}H NMR spectroscopy, the benzene ligand in the rhodium complex **3a** is completely replaced by acetone-d_6 within 0.5 h (2 h for **1a**). The iridium analogue **4a** is decomposed by acetonitrile-d_3 within 4 h, whereas **2a** remains unchanged after 1 week. The greater reactivity of the metallacarborane complexes is apparently connected with higher π-acceptor ability of the carborane ligand $[9\text{-}SMe_2\text{-}7,8\text{-}C_2B_9H_{10}]^-$ compared to Cp^- (vide infra).

We found that rhodacarborane complexes **3** are able to undergo arene exchange reactions, similar to the related pentamethylcyclopentadienyl complexes $[Cp^*Rh(C_6H_6)]^{2+}$ and $[Cp^*Ir(C_{10}H_8)]^{2+}$ [14, 15]. As a matter of fact, refluxing of the benzene complex **3a** in nitromethane in the presence of anisole during 2 h leads to complex **3f**. It is noteworthy, that this reaction proceeds even at a room temperature but with much lower rate: according to ^{1}H NMR spectroscopy, the degree of conversion is about 56% after 1 week. On the contrary, the iridium analogue **4a** does not react with anisole in refluxing nitromethane even in the presence of catalytic quantities of acetonitrile.

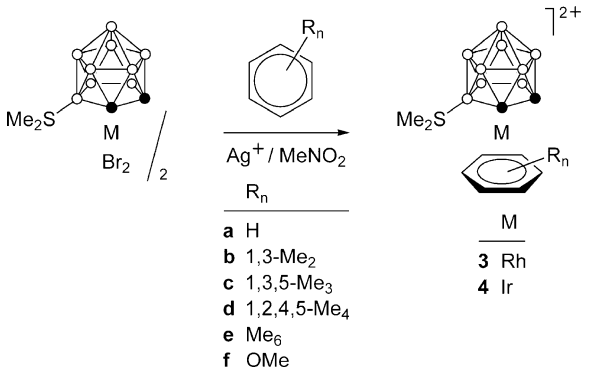

Scheme 3 Synthesis of the metallacarborane arene complexes **3** and **4**

As in the case of **1**, **2**, and $[(\eta\text{-}7,8\text{-}Me_2\text{-}7,8\text{-}C_2B_9H_{11})Rh(arene)]^+$ [3, 16], in the ^{1}H NMR spectra of complexes **3** and **4**, the signals for the arene ring protons undergo downfield shift with respect to the free arene, Table 1, as a consequence of a high positive charge whose effect overrides the opposite effect of coordination to the transition metal atom. Moreover, for metallacarborane complexes **3**, **4**, and $[(\eta\text{-}7,8\text{-}Me_2\text{-}7,8\text{-}C_2B_9H_{11})Rh(arene)]^+$, these signals are more downfield shifted than for the cyclopentadienyl analogues, possibly owing to the stronger acceptor effect of a carborane ligand. The observed double set of the methyl group signals for the 1,3-xylene complexes **3b** and **4b** can be explained by C_1 symmetry of the complexes [13].

X-ray structure of complex **4f**$(BF_4)_2$

The structure of **4f**$(BF_4)_2$ was determined by X-ray diffraction, Fig. 1. Cation **4f** is the first crystallographically characterized dicationic metallacarborane. The methoxy group is disordered over two sites with the site occupancy factors equal to 0.695 and 0.305. The angle between the C_6 and C_2B_3 planes is equal to 6.9°, possibly owing to steric effect of the SMe_2 group. The shortest intramolecular nonbonding distances C11−S1 (3.527(6) Å) and C12−S1 (3.634(6) Å) are essentially less than the sum of Van der Waals radii of the C and S atoms (3.94 Å). The Ir···C_2B_3 distance in **4f** (1.586(4) Å) is very close to that in the Cp* complex $[(\eta\text{-}9\text{-}SMe_2\text{-}7,8\text{-}C_2B_9H_{10})IrCp^*]^+$ (1.598 Å) [11].

Electrochemistry

Figure 2 compares the cyclic voltammetric responses exhibited in MeCN solution by $[\mathbf{1a}]^{2+}$ and $[\mathbf{1e}]^{2+}$, respectively.

At low scan rates, both the complexes display a series of reduction processes with features of chemical irreversibility and different peak heights. In both cases, the most cathodic processes tend to decrease with the scan rate, thus indicating that they arise from chemical complications accompanying the first main reduction. In the case of $[\mathbf{1a}]^{2+}$, the first reduction does not exhibit any directly associated return peak even at the highest scan rate (51.2 V s^{-1}), whereas in the case of the arene-permethylated analogue $[\mathbf{1e}]^{2+}$, the progressive increase in the scan rate makes the directly associated return peak to increase progressively (at 51.2 V s^{-1} the i_{pa}/i_{pc} ratio is around 0.7). Assuming that a first-order chemical complication is operative (in fact, no appreciable differences were noted in the concentration range from 0.3×10^{-3} mol dm^{-3} to 1.0×10^{-3} mol dm^{-3}), a half-life of 0.01 s can be estimated for the arene η^6 coordinated Rh(II) monocation $[\mathbf{1e}]^+$ [17], or a lifetime markedly lower than that estimated in acetone solution for the cyclopentadienyl-permethylated analogue (about 1,800 s at 261 K) [2].

Table 1 [1]H NMR spectroscopic data for complexes **3** and **4** in nitromethane-d_3[a]

Complex	SMe_2	CH cage	Arene
3a	2.91 (s, 6H)	5.76 (bs, 1H), 6.36 (bs, 1H)	8.03 (s, 6H, C_6H_6)
3b	2.91 (s, 6H)	5.41 (bs, 1H), 6.17 (bs, 1H)	7.78 (m, 1H, $C_6H_4Me_2$), 7.74 (s, 1H, $C_6H_4Me_2$), 7.69 (m, 2H, $C_6H_4Me_2$), 2.83 (s, 3H, $C_6H_4Me_2$), 2.77 (s, 3H, $C_6H_4Me_2$)
3c	2.92 (s, 6H)	5.22 (bs, 1H), 6.00 (bs, 1H)	7.57 (s, 3H, $C_6H_3Me_3$), 2.77 (s, 9H, $C_6H_3Me_3$)
3d	2.91 (s, 6H)	5.33 (bs, 1H), 5.76 (bs, 1H)	7.53 (s, 2H, $C_6H_2Me_4$), 2.69 (s, 6H, $C_6H_2Me_4$), 2.67 (s, 6H, $C_6H_2Me_4$)
3e	2.87 (s, 3H), 2.85 (s, 3H)	4.72 (bs, 1H), 5.58 (bs, 1H)	2.67 (s, 18H, C_6Me_6)
3f	2.88 (s, 6H)	5.59 (bs, 1H), 6.20 (bs, 1H)	7.81 (m, 2H, C_6H_5OMe), 7.67 (m, 3H, C_6H_5OMe), 4.40 (s, 3H, C_6H_5OMe)
4a	2.86 (s, 6H)	5.86 (bs, 1H), 6.49 (bs, 1H)	8.03 (s, 6H, C_6H_6)
4b	2.87 (s, 3H), 2.86 (s, 3H)	5.51 (bs, 1H), 6.31 (bs, 1H)	7.80 (m, 3H, $C_6H_4Me_2$), 7.71 (m, 1H, $C_6H_4Me_2$), 2.94 (s, 3H, $C_6H_4Me_2$), 2.88 (s, 3H, $C_6H_4Me_2$)
4c	2.91 (s, 3H), 2.87 (s, 3H)	5.32 (bs, 1H), 6.15 (bs, 1H)	7.67 (s, 3H, $C_6H_3Me_3$), 2.89 (s, 9H, $C_6H_3Me_3$)
4d	2.89 (s, 3H), 2.87 (s, 3H)	5.50 (bs, 1H), 5.91 (bs, 1H)	7.60 (s, 2H, $C_6H_2Me_4$), 2.76 (s, 12H, $C_6H_2Me_4$)
4e	2.85 (s, 6H)	4.88 (bs, 1H), 5.80 (bs, 1H)	2.72 (s, 18H, C_6Me_6)
4f	2.86 (s, 3H), 2.84 (s, 3H)	5.71 (bs, 1H), 6.36 (bs, 1H)	7.78 (m, 5H, C_6H_5OMe), 4.42 (s, 3H, C_6H_5OMe)

[a] Chemical shifts in ppm

It is noted that, in both cases, independently from the electrode material (platinum or gold), rather severe electrode poisoning processes made necessary the mechanical cleaning of the electrode surface after each voltammetric cycle. Even if such a drawback makes uncertain the ascertainment of the number of electrons involved in the main cathodic step by controlled potential coulometry, it has been found that after the consumption of about 0.5 electrons/molecule the original golden-yellow solutions of the two derivatives turn red in the case of $[\mathbf{1a}]^{2+}$ (E_w=−0.3 V, vs SCE) and pinky-brown in the case of $[\mathbf{1e}]^{2+}$ (E_w=−0.4 V) and again golden-yellow after about 1 electron (in spite of the persistent presence of minor residual currents, the electrolysis process was interrupted because of the need of continuous renewal of the electrode surface). As a matter of fact, the resulting solutions no more afford well-defined redox profiles.

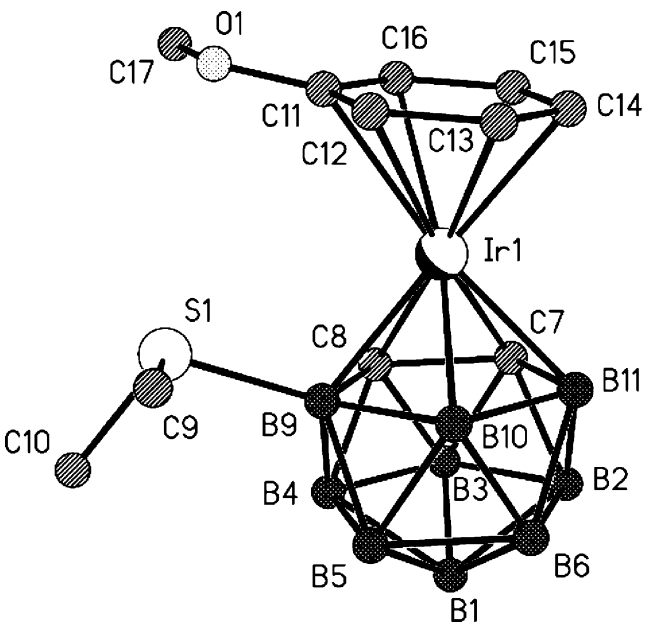

Fig. 1 X-ray structure of cation **4f**. Selected distances (Å): Ir1−C7 2.161(5), Ir1−C8 2.170(5), Ir1−C11 2.328(3), Ir1−C12 2.258(3), Ir1−C13 2.196(3), Ir1−C14 2.205(3), Ir1−C15 2.277(3), Ir1−C16 2.337(3), Ir1−B9 2.184(6), Ir1−B10 2.193(6), Ir1−B11 2.186(6), B9−S1 1.914(6), Ir1···C_2B_3 1.586(4), Ir1···C_6H_5 1.785(3)

In reality, it was quite useful to look at the minor reversible asterisked peak system after the first reduction in $[\mathbf{1e}]^{2+}$, which, being reminiscent of that exhibited by such dication in the same solvent at low temperature, and that exhibited by the wider family $[(C_6R_6)RhCp^*]^{2+}$ in acetone solution [2], could represent the effective Rh(II)/Rh(I) reduction $[\mathbf{1e}]^{+/0}$ of the original Rh(III) derivative. In confirmation, Fig. 3a,b shows how the pertinent cyclic voltammetric profile changes with the scan rate.

It is evident that the increase in the scan rate causes a progressive increase in the second process. In fact, at the highest scan rate, the graphically measured current ratio between the two processes, $i_{pc(II)}/i_{pc(I)}$, is about 0.8–0.9, indicating the almost complete prevention of the chemical complication after the generation of the monocation Rh(II) $[\mathbf{1e}]^{+}$. Based on the fact that the current function $i_{pc}xv^{-1/2}$ of

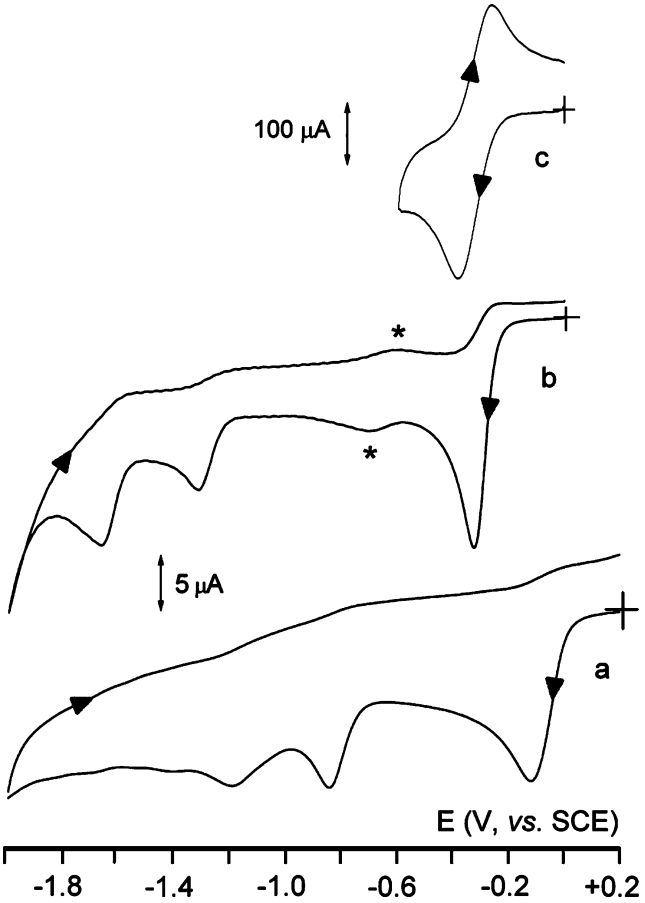

Fig. 2 Cyclic voltammograms recorded at a platinum electrode in MeCN solution of: **a** $[\mathbf{1a}]^{2+}$ (1.1×10^{-3} mol dm^{-3}); **b**, **c** $[\mathbf{1e}]^{2+}$ (0.8×10^{-3} mol dm^{-3}). $[NBu_4][PF_6]$ (0.2 mol dm^{-3}) supporting electrolyte. Scan rates: **a**, **b** 0.2 V s^{-1}; **c** 51.2 V s^{-1}

the first process decreases by less than 10% for each ten time increase in the scan rate, the occurrence of a electrochemical–chemical (EC) mechanism over a electrochemical–chemical–electrochemical [ECE; or electrochemical–electrochemical–chemical (EEC)] mechanism is preferred [17], in agreement, on the other hand, with the one-electron involvement measured in the longer time scales of controlled potential coulometry.

As illustrated in Fig. 3c,d, just a similar behavior is exhibited by $[\mathbf{1e}]^{2+}$ in PC solution, which means that no beneficial effects on the stability of the Rh(II) monocation $[\mathbf{1e}]^{+}$ ($t_{1/2}\approx0.01$ s) are played by the PC solvent with respect to MeCN.

In contrast, a slight stabilization of the arene η^6 coordinated Rh(II) monocation $[\mathbf{1a}]^{+}$ seems to be given by the PC solvent. In fact, not only a very slight, directly associated, return peak to the Rh(III)/Rh(II) step $[\mathbf{1a}]^{2+/+}$ tends to appear at the highest scan rates but also the Rh(II)/Rh(I) reduction $[\mathbf{1a}]^{+/0}$ becomes detectable.

At any rate, in confirmation of the fast kinetics of the associated chemical complications, the decrease in the temperature to 253 K does not significantly improve the stability of the monocation $[\mathbf{1a}]^{+}$.

The elusive nature of the Rh(II)/Rh(I) process in these complexes as a function of the solvent is further confirmed by comparison of the cyclic voltammetric behavior of $[Cp^*Rh(\eta^6\text{-}C_6H_6)]^{2+}$ in PC solution with that previously reported in acetone solution, where great difficulties were encountered in determining the mentioned second reduction [2]. As illustrated in Fig. 4, in PC solution, both the steps are clearly detectable at high scan rates, even if the Rh(II) monocation still maintains very short lived.

Passing to the Ir(III) complexes $[\mathbf{2a}]^{2+}$ and $[\mathbf{2e}]^{2+}$, they afford the expected single (two-electron) reduction [1]. As illustrated in Fig. 5, which refers to the pertinent responses in MeCN solution, also in this case, the chemical reversibility of the reduction in the arene permethylated

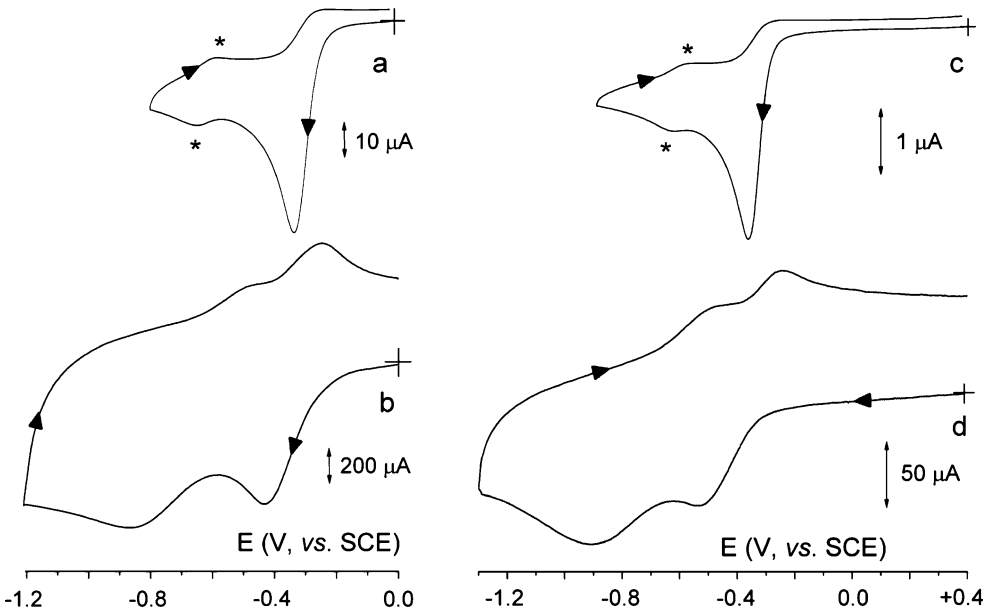

Fig. 3 Cyclic voltammograms recorded at a platinum electrode in: **a**, **b** MeCN solution of $[\mathbf{1e}]^{2+}$ (1.2×10^{-3} mol dm^{-3}); **c**, **d** PC solution of $[\mathbf{1e}]^{2+}$ (0.7×10^{-3} mol dm^{-3}). $[NBu_4][PF_6]$ (0.2 mol dm^{-3}) supporting electrolyte. Scan rates: **a**, **c** 0.05 V s^{-1}; **b**, **d** 51.2 V s^{-1}

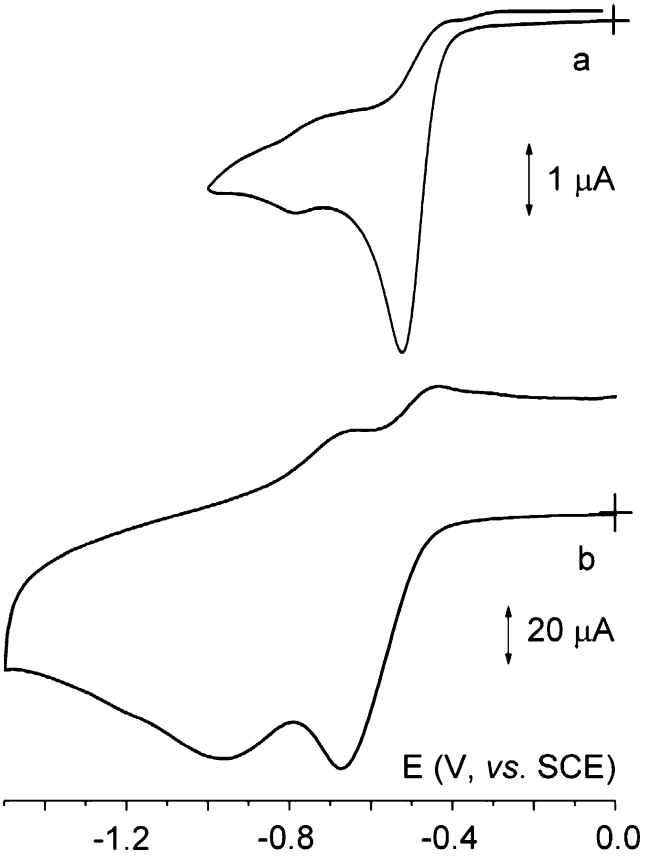

Fig. 4 Cyclic voltammograms recorded at a platinum electrode in PC solution of $[Cp^*Rh(\eta^6\text{-}C_6H_6)]^{2+}$ (1.8×10^{-3} mol dm^{-3}). $[NBu_4][PF_6]$ (0.2 mol dm^{-3}) supporting electrolyte. Scan rates: **a** 0.05 V s^{-1}; **b** 34.1 V s^{-1}. T=298 K

complex is higher, but still partial, than that of the unsubstituted analogue. Such finding contrasts with the chemical reversibility of the reduction in the completely permethylated $[Cp^*M(\eta^6\text{-}C_6Me_6)]^{2+}$ [1].

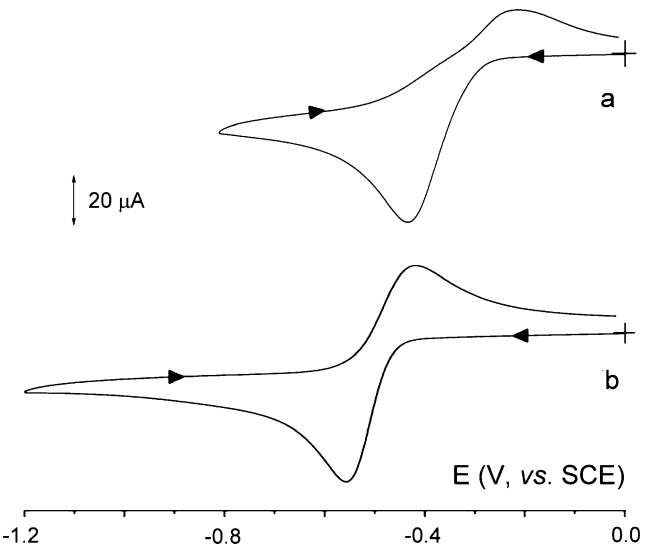

Fig. 5 Cyclic voltammograms recorded at a gold electrode in MeCN solution of: **a** $[\mathbf{2a}]^{2+}$ (0.7×10^{-3} mol dm^{-3}); **b** $[\mathbf{2e}]^{2+}$ (0.8×10^{-3} mol dm^{-3}). $[NBu_4][PF_6]$ (0.2 mol dm^{-3}) supporting electrolyte. Scan rate 0.1 V s^{-1}

The evaluation of the lifetimes of the Ir(I) neutral species $[\mathbf{2a}]^0$ and $[\mathbf{2e}]^0$ leads to 2 and 15 s, respectively.

A similar behavior was obtained in PC solution, even if the chemical reversibility of the reduction process of $[\mathbf{2e}]^{2+}$ is slightly improved, leading to a lifetime of 30 s for the corresponding neutral species.

Let us now pass to the Rh(III)-monoanionic carborane complexes.

Figure 6a–c illustrates the cyclic voltammetric behavior of a MeCN solution just after the dissolution of $[\mathbf{3a}]^{2+}$ at −20 °C (a, b) and at +25 °C (c), respectively.

It apparently exhibits two main reduction processes A, D, which are coupled to the minor processes B, C, and E. In reality, upon increasing the scan rate, peak D is progressively replaced by peak C, thus suggesting that the sequence $[\mathbf{3a}]^{2+/+/0}$ is given by peaks A and C, whereas peaks B, D, and E are due to the new species arising from the molecular reorganization of $[\mathbf{3a}]^{2+}$ in MeCN. In confirmation, at room temperature, only peaks B and D are substantially detected. In this connection, the disappearance of peak A at room temperature suggests that a preceding reversible chemical reaction is also operative (plausibly, the arene replacement for MeCN molecules).

Apart from minor details, a similar behavior is exhibited by $[\mathbf{3a}]^{2+}$ in PC solution, which means that $[\mathbf{3a}]^{+}$ is very short-lived also in PC solution. In short, at low scan rates, it apparently exhibits the separate sequence Rh(III)/Rh(II)/Rh(I). Nevertheless, the second step tends to disappear with the increase in the scan rate, so that it cannot be assigned to the Rh(II)/Rh(I) process $[\mathbf{3a}]^{+/0}$. In reality, as happens for complexes $[\mathbf{1a}]^{2+}$ and $[\mathbf{1e}]^{2+}$, the increase in the scan rate makes the $[\mathbf{3a}]^{+/0}$ reduction to appear (at potential values less negative than the reduction in the by-product originated in correspondence of the first step), Fig. 6d.

In contrast, in agreement with the cited beneficial effects of arene methylation, less complicate appears the voltammetric behavior of $[\mathbf{3c}]^{2+}$ either in MeCN or PC solution, Fig. 7.

In fact, in MeCN, the voltammetric picture is constituted by two, substantially irreversible, reductions, the extent of reversibility of which does not appreciably vary with the increase in the scan rate (but for the second process which is slightly split at the highest rates). As expected, controlled potential coulometry in correspondence of the first reduction (E_w=−0.1 V) consumes one electron/molecule. In confirmation of the occurrence of chemical complications, during the exhaustive electrolysis, the original pale yellow solution turns progressively green, black, and red, and the final solution no more displays in cyclic voltammetry the residues of the original profile as well as that of identifiable by-products.

In PC solution, however, the two reductions display features of marked reversibility, even if the analysis of the

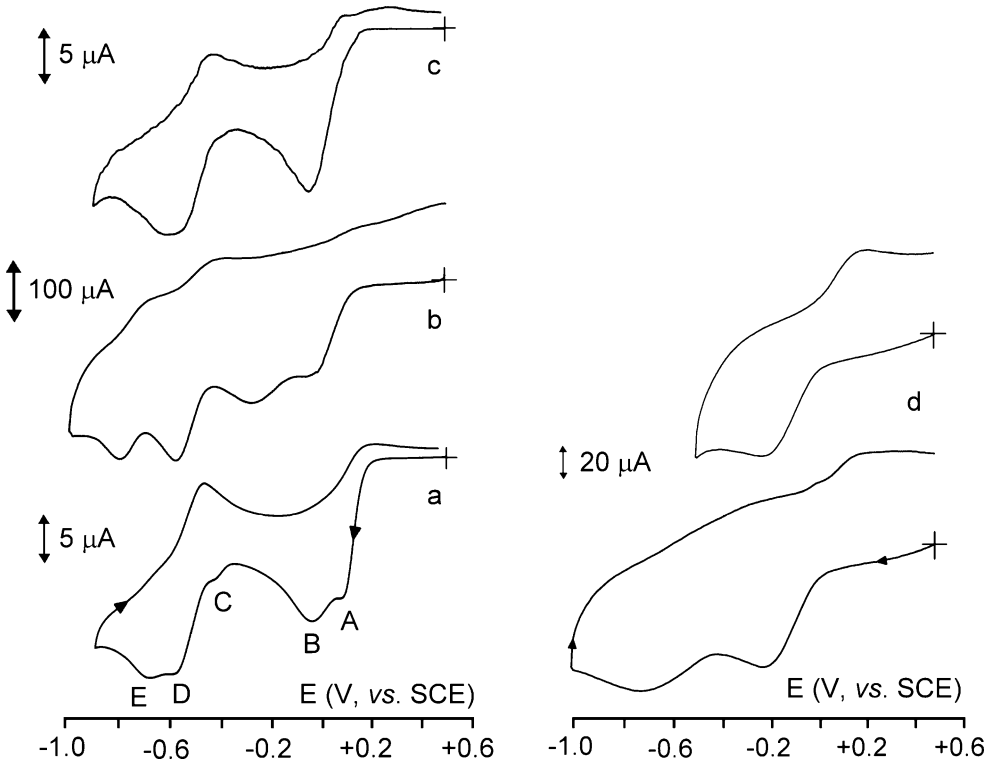

Fig. 6 Cyclic voltammograms recorded at a platinum electrode in: **a**–**c** MeCN solution of $[\mathbf{3a}]^{2+}$ (1.0×10^{-3} mol dm^{-3}) at 253 K (**a**, **b**) and 298 K (**c**), respectively; **d** PC solution of $[\mathbf{3a}]^{2+}$ (0.8×10^{-3} mol dm^{-3}). T=253 K. $[NBu_4][PF_6]$ (0.2 mol dm^{-3}) supporting electrolyte. Scan rates: **a**, **c** 0.2 V s^{-1}; **b**, **d** 51.2 V s^{-1}

cyclic voltammetric responses, at low scan rates, still indicates the presence of slow chemical complications. In fact, a lifetime of about 20 s is calculated for the arene η^6 coordinated Rh(II) monocation $[\mathbf{3c}]^{+}$.

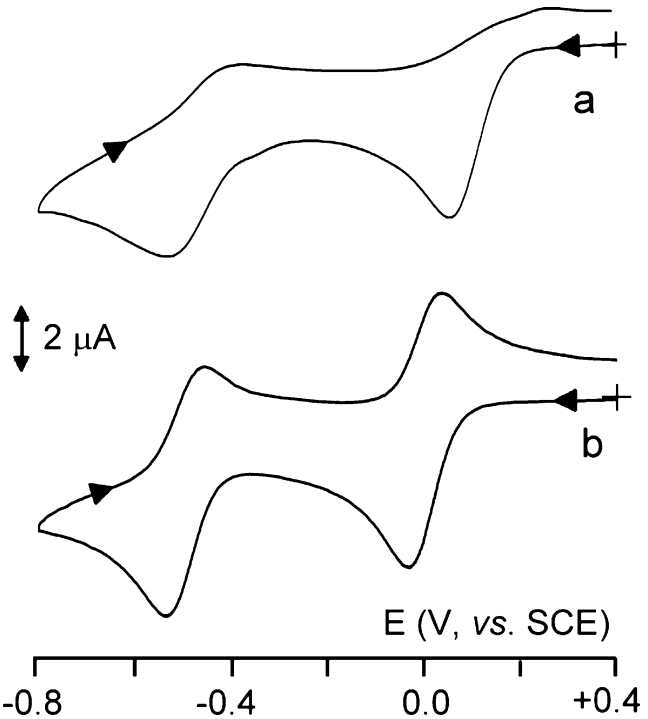

Fig. 7 Cyclic voltammograms exhibited at a platinum electrode by $[\mathbf{3c}]^{2+}$ (0.8×10^{-3} mol dm^{-3}) in: **a** MeCN solution; **b** PC solution. $[NBu_4][PF_6]$ (0.2 mol dm^{-3}) supporting electrolyte. Scan rate 0.2 V s^{-1}

Testifying to the fact that the stability in solution of the reduction products of the present complexes is also a function of intrinsic electronic effects, the dication $[\mathbf{3f}]^{2+}$, both in MeCN and PC solutions, gives rise to two reductions, only the second of which shows limited chemical reversibility.

It is, however, noted that, at room temperature, the pale yellow PC solution of $[\mathbf{3f}]^{2+}$ slowly tends to become green, thus suggesting that the true reduction path can be more reliably determined at low temperature.

As a matter of fact, as illustrated in Fig. 8, the low temperature voltammetric pattern is rather complex, in that at low scan rate, the previous (deceiving) two sequential reductions A and C appear. The increase in the scan rate makes the reduction C to disappear in favor of the reduction B, but the further increase in the scan rate proves that also this latter is due to a short-lived byproduct and that the Rh(II)/Rh(I) step $[\mathbf{3f}]^{+/0}$ corresponds to peak D.

Finally, Fig. 9 compares the cyclic voltammetric responses of $[\mathbf{4a}]^{2+}$ and $[\mathbf{4c}]^{2+}$ in MeCN solution.

As in the case of $[\mathbf{2a}]^{2+}$ and $[\mathbf{2e}]^{2+}$, the arene methylation in $[\mathbf{4c}]^{2+}$ improves the chemical reversibility of the Ir(III)/Ir

Fig. 8 Cyclic voltammograms recorded at a platinum electrode in ▶ PC solution of $[\mathbf{3f}]^{2+}$ (1.8×10^{-3} mol dm^{-3}) at 253 K. $[NBu_4][PF_6]$ (0.2 mol dm^{-3}) supporting electrolyte. Scan rates: **a** 0.02 V s^{-1}; **b** 0.2 V s^{-1}; **c** 1.0 V s^{-1}; **d** 20.48 V s^{-1}; **e**, **f** 51.2 V s^{-1}

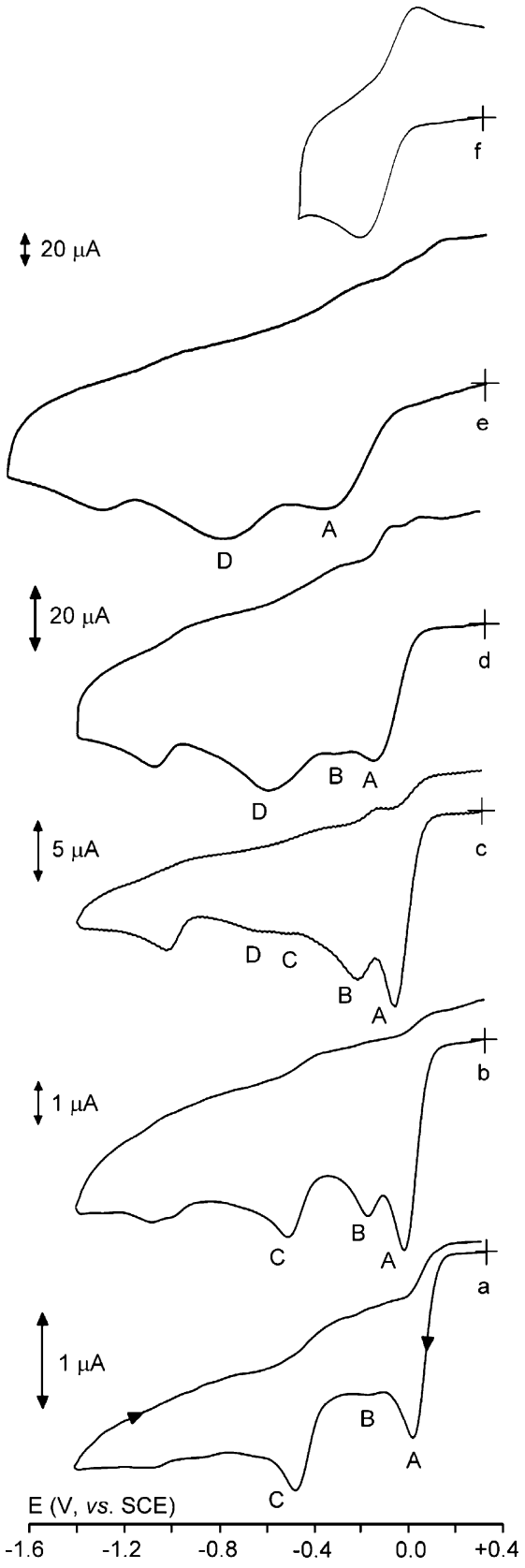

(I) process (or, the stability of the Ir(I) species). In fact, half-lives of 2 and 18 s can be calculated for $[\mathbf{4a}]^0$ and $[\mathbf{4c}]^0$, respectively (under the usual assumption of first-order chemical complications). In both cases, further reduction processes are present at more negative potentials, which, tending to disappear with the increase in the scan rate, are attributed to the chemical complications after the main electron transfer. On the other hand, the lifetime of $[\mathbf{4f}]^0$ is even shorter than that of $[\mathbf{4a}]^0$.

Unexpectedly, no improvement of the relative stability of the electro-generated $[\mathbf{4a}]^0$, $[\mathbf{4c}]^0$, $[\mathbf{4f}]^0$ Ir(I) derivatives has been gained in PC solution.

The formal electrode potentials of the studied $[(\eta^5\text{-}C_5R_5)M(\eta^6\text{-}C_6R_6)]^{2+}$ and $[(\eta\text{-}9\text{-}SMe_2\text{-}7,8\text{-}C_2B_9H_{10})M(\eta^6\text{-}C_6R_6)]^{2+}$ complexes are summarized in Table 2.

As deducible, the complexes of the monoanionic carborane ligands are more easily reduced than the cyclopentadienyl analogues, thus confirming that $[9\text{-}SMe_2\text{-}7,8\text{-}C_2B_9H_{10}]^-$ is markedly less electron donating than $[C_5R_5]^-$ [10].

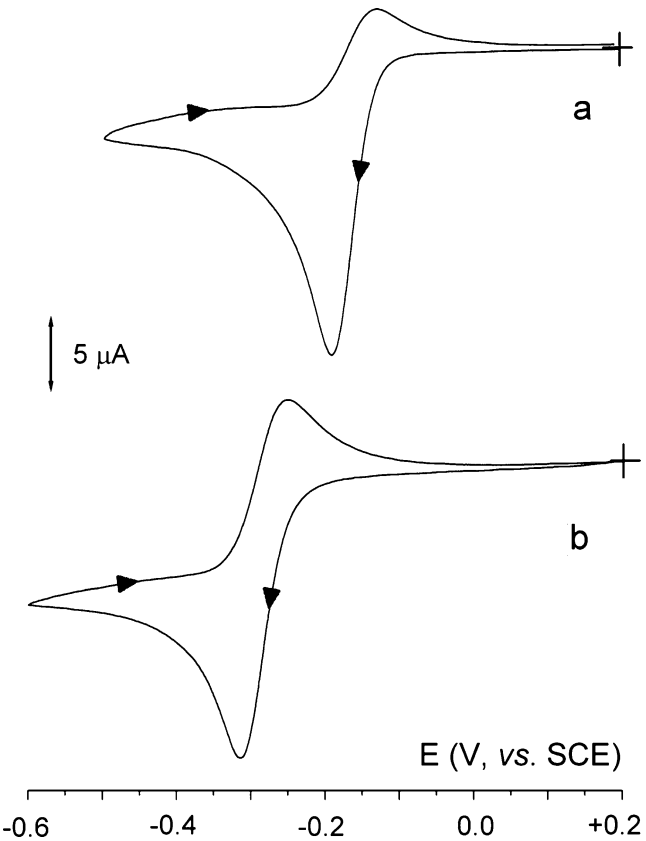

Fig. 9 Cyclic voltammograms recorded at a platinum electrode in MeCN solution of: **a** $[\mathbf{4a}]^{2+}$ (1.0×10^{-3} mol dm^{-3}); **b** $[\mathbf{4c}]^{2+}$ (1.2×10^{-3} mol dm^{-3}). $[NBu_4][PF_6]$ (0.2 mol dm^{-3}) supporting electrolyte. Scan rate 0.02 V s^{-1}

Table 2 Formal electrode potentials (V, vs SCE) and peak-to-peak separation (mV) for the main reduction processes exhibited by the Rh(III) and Ir(III) complexes in different solvents

Complex	$E^{\circ\prime}$ (1st reduction)	ΔE_p	$E^{\circ\prime}$ (2nd reduction)	ΔE_p	Solvent	Temperature (K)
$[\mathbf{1a}]^{2+}$	−0.16[a,b]	–	Not detected	–	MeCN	298
	−0.20[c,d]	240[c,d]	−0.54[c,d]	350[c,d]	PC	298
	−0.27[c,d]	330[c,d]	−0.58[c,d]	520[c,d]	PC	253
$[\mathbf{1e}]^{2+}$	−0.30	76[e]	−0.64	145[e]	MeCN	298
	−0.36	83[e]	−0.64	104[e]	PC	298
	−0.35[f]	–	−0.63[f]	–	MeCN	261
$[Cp^*Rh(C_6H_6)]^{2+}$	−0.56[c]	256[c]	−0.82[c,d]	350[c,d]	PC	298
	−0.62[c]	236[c]	−1.16[b,c]	410[c,d]	PC	253
	−0.48[f]	–	–	–	Me_2CO	298
$[\mathbf{2a}]^{2+}$	−0.32[g]	217[a]	–	–	MeCN	298
	−0.35[g]	220[a]	–	–	PC	298
$[\mathbf{2e}]^{2+}$	−0.49[g]	148	–	–	MeCN	298
	−0.51[g]	173	–	–	PC	298
$[\mathbf{3a}]^{2+}$	+0.08[a,b]	–	−0.49	176[c,d]	MeCN	253
	−0.04[a,b,h]	–	−0.46[h]	116[c,d]	MeCN	298
	−0.02[c]	384[c]	−0.48	440[c,d]	PC	253
	−0.03	110[c]	−0.39	270[c,d]	PC	298
$[\mathbf{3c}]^{2+}$	+0.12[i]	154[a]	−0.47[i]	129[a]	MeCN	298
	0.00[h]	66[a]	−0.50[i]	78[a]	PC	298
	−0.05	58[a]	−0.52	98[a]	PC	253
$[\mathbf{3f}]^{2+}$	+0.04[a,b]	–	−0.54[i]	117[a]	MeCN	298
	+0.03[a,b]	–	−0.45[a,b]	–	PC	298
	−0.08[c]	212[c]	-0.50[c]	560[c,d]	PC	253
$[\mathbf{4a}]^{2+}$	−0.16[g]	92	–	–	MeCN	298
	−0.3[l]	–	–	–	PC	298
$[\mathbf{4c}]^{2+}$	−0.28[g]	104	–	–	MeCN	298
	−0.32[g]	88	–	–	PC	298
$[\mathbf{4f}]^{2+}$	−0.23[a,b,g]	–	–	–	MeCN	298
	−0.24[g,i]	120[a]	–	–	PC	298

[a] Measured at 0.2 V s^{-1}
[b] Peak potential value for irreversible processes
[c] Measured at 51.2 V s^{-1}
[d] Rough evaluation (see text)
[e] Measured at 2.0 V s^{-1}
[f] From [2]
[g] Two-electron process
[h] Decomposition product (see text)
[i] Partially chemically reversible
[l] Ill defined

Conclusions

In agreement with previous findings [1, 2], we have proved that the reduction path of the complexes $[CpM^{III}(\eta^6\text{-}C_6R_6)]^{2+}$ (M=Rh, Ir; R=H, Me) is highly dependent on both the nature of the solvent and the intrinsic electronic properties of the arene substituents. We have, however, shown that the use of propylene carbonate can improve the reversibility of the pertinent M(III)/M(II)/M(I) sequences or to increase the lifetime of the complexes in their lower oxidation states before changing the arene coordination from η^6 to η^4. As expected from the analogy between Cp^- and $[9\text{-}SMe_2\text{-}7,8\text{-}C_2B_9H_{10}]^-$, complexes $[(\eta\text{-}9\text{-}SMe_2\text{-}7,8\text{-}C_2B_9H_{10})M^{III}(\eta^6\text{-}C_6R_6)]^{2+}$ (C_6R_6=C_6H_6, C_6H_5OMe, $C_6H_3Me_3$) substantially behave in a similar manner.

Acknowledgements The financial support of the University of Siena (PAR 2005; P.Z.) and of the Division of General Chemistry and Material Sciences of RAS (A.R.K) is gratefully acknowledged.

References

1. Bowyer WJ, Geiger WE (1985) J Am Chem Soc 107:5657
2. Bowyer WJ, Merkert JW, Geiger WE, Rheingold AL (1989) Organometallics 8:191
3. Loginov DA, Vinogradov MM, Starikova ZA, Petrovskii PV, Kudinov AR (2004) Russ Chem Bull 53:1949 (and references therein)
4. Koelle U, Fuss B, Rajasekharan MV, Ramakrishna BL, Ammeter JH, Böhm MC (1984) J Am Chem Soc 106:4152
5. Kudinov AR, Perekalin DS, Petrovskii PV, Lyssenko KA, Grintselev-Knyazev GV, Starikova ZA (2002) J Organomet Chem 657:115
6. Kudinov AR, Perekalin DS, Petrovskii PV (2001) Russ Chem Bull 50:1334
7. Woodhouse ME, Lewis FD, Marks TJ (1982) J Am Chem Soc 104:5586
8. Fabrizi de Biani F, Corsini M, Zanello P, Yao H, Bluhm ME, Grimes RN (2004) J Am Chem Soc 126:11360
9. Kudinov AR, Perekalin DS, Petrovskii PV, Grintselev-Knyazev GV (2002) Russ Chem Bull 51:1928
10. Meshcheryakov VI, Kitaev PS, Lyssenko KA, Starikova ZA, Petrovskii PV, Janoušek Z, Corsini M, Laschi F, Zanello P, Kudinov AR (2005) J Organomet Chem 690:4745
11. Loginov DA, Vinogradov MM, Perekalin DS, Starikova ZA, Lyssenko KA, Petrovskii PV, Kudinov AR (2006) Russ Chem Bull 55:84
12. Kudinov AR, Meshcheryakov VI, Petrovskii PV, Rybinskaya MI (1999) Russ Chem Bull 48:1794
13. Loginov DA, Muratov DV, Starikova ZA, Petrovskii PV, Kudinov AR (2006) J Organomet Chem 691:3646
14. Kaganovich VS, Kudinov AR, Rybinskaya MI (1986) Bull Acad Sci USSR Div Chem Sci 35:2418
15. Kaganovich VS, Kudinov AR, Rybinskaya MI (1988) Organomet Chem USSR 1:162
16. Kudinov AR, Bogoudinov RT, Petrovskii PV, Rybinskaya MI (1999) Russ Chem Bull 48:586
17. Zanello P (2003) Inorganic electrochemistry. Theory, practice and application. RSC, Oxford